EKSPLOATACJA I NIEZAWODNOŚĆ MAINTENANCE AND RELIABILITY

Eksploatacja i Niezawodnosc – Maintenance and Reliability

Volume 24 (2022), Issue 1

journal homepage: http://www.ein.org.pl

Article citation info:
Nowakowski T, Komorski P. Diagnostics of the drive shaft bearing based on vibrations in the high-frequency range as a part of the vehicle's self-diagnostic system. Eksploatacja i Niezawodnosc – Maintenance and Reliability 2022; 24 (1): 70–79, http://doi.org/10.17531/ein.2022.1.9.

Diagnostics of the drive shaft bearing based on vibrations in the high-frequency range as a part of the vehicle's self-diagnostic system

Indexed by: Web of Science Group

Tomasz Nowakowski [a], Pawel Komorski [a,*]

[a] Poznan University of Technology, Faculty of Civil and Transport Engineering, Institute of Transport, ul. Piotrowo 3, 61-138 Poznań, Poland

Highlights

- Vibration measurements of the drive shaft bearings in selected vehicle during operation.
- Vibration signal processing and analysis in time and frequency domains.
- Selection of the most sensitive diagnostic parameter based on decision trees.
- On-board diagnostic algorithm to assess the technical condition of drive shaft bearings.

Abstract

Currently, one of the trends in the automotive industry is to make vehicles as autonomous as possible. In particular, this concerns the implementation of complex and innovative self-diagnostic systems for cars. This paper proposes a new diagnostic algorithm that evaluates the performance of the drive shaft bearings of a road vehicle during use. The diagnostic parameter was selected based on vibration measurements and machine learning analysis results. The analyses included the use of more than a dozen time domain features of vibration signal in different frequency ranges. Upper limit values and down limit values of the diagnostic parameter were determined, based on which the vehicle user will receive information about impending wear and total bearing damage. Additionally, statistical verification of the developed model and validation of the results were performed.

Keywords

self-diagnostic system, vibration, vehicles, signal processing methods, decision trees.

1. Introduction

An important issue that is part of the scientific field of machine operation is technical diagnostics, which consists in assessing the technical condition of a machine without disassembling it [9, 25]. For this purpose, most often working and/or accompanying processes during the operation of a technical object are used for testing [9, 30, 35]. This type of approach to condition monitoring is particularly used during the operation of various types of road vehicles [29, 32], rail vehicles [11, 26], aircrafts [2, 31] and industrial machinery [6, 18]. Technical components that are particularly susceptible to damage are rotating elements (e.g. bearings, gears, rotors, shafts, etc.). These systems or elements are often exposed to high loads and unfavorable working conditions. In order not to lead to a bad technical condition of the object, their work should be monitored in real time during the operation.

The concept of self-diagnosing vehicles, especially in the automotive industry, is particularly prominent. The origin of OBD systems dates back to the 1970s and 1980s [24]. The essence of OBD systems is the rapid diagnosis of malfunctions that have an adverse effect on the environment. However, the notion of diagnostics may refer to many other factors affecting the technical condition of a vehicle from a broader point of view, i.e. comfort and safety of driving or prediction of repair costs. In the last dozen or so years, the development of this area has been accelerated, and the biggest car corporations outdo each other in terms of developing innovative solutions. The use of various types of sensors (e.g. pressure, temperature, vibrations, etc.), actuators and filters in mechanical systems (e.g. fuel injection, exhaust gas cleaning, etc.), and, most of all, electrical and electronic systems in modern vehicles is not surprising as regards technical condition monitoring and emission testing [17]. One of the many examples of on-board diagnostic systems is the use of noise emissivity to monitor the condition of air-conditioner blower operation using the artificial neural network technique [39]. Another example is the use of pressure change signal as a diagnostic parameter to monitor vehicle tires [32]. The research led to the development of a low cost piezoresistive sensing method based on smart pressure sensor which achieves greater accuracy due to its built-in temperature compensation, filtering and self-calibration capabilities. A recent example of an on-board diagnostic system is a proposal for a tool to monitor the performance of battery systems in electric vehicles (vehicles that are becoming increasingly popular these days) [42]. The system is based on big data statistical methods (machine learning algorithms) using the changes of cell terminal voltages in a battery pack as the main diagnostic parameter. In addition to monitoring vehicle performance, research is also being carried out to analyze driver behavior as one of the main sources of danger on the roads and also the main culprit for some vehicle damage and malfunctions, which may result from improper use and driving style [4]. In conclusion, it is worth noting that the common part of most of the above-mentioned research and

(*) Corresponding author.

E-mail addresses: T. Nowakowski (ORCID: 0000-0001-5415-7052): tomasz.nowakowski@put.poznan.pl, P. Komorski (ORCID: 0000-0003-3213-3855): pawel.komorski@put.poznan.pl

analysis is the use of machine learning algorithms as an effective tool of artificial intelligence in the development of various types of on-board diagnostic systems. Another example of adaptation of machine learning algorithm to the kind and type of malfunction of the throttle control subsystem in a car is the research described in the [29]. On the other hand, the paper [37] presents an extensive literature analysis on the use of artificial intelligence in the diagnostics of various systems/assemblies in a vehicle.

This paper presents a modern approach to monitoring the performance of drive shaft bearings in a road vehicle. Vibration accelerations of a drive shaft bearing in good and bad technical condition were measured. The analyses involved various time domain features of vibration signal over several frequency ranges. Thus, the vibration signal was used as the main diagnostic parameter, using machine learning to develop a new algorithm for diagnosing drive shaft bearings as part of a comprehensive car self-diagnostic system (CSDS). The system is ultimately intended to complement OBD-type systems with information related to predicting operating costs. Permissible and limiting values of the selected diagnostic parameter have been indicated. Additionally, the regression model of the diagnostic parameter as a function of the driving speed has been developed, validated and statistically verified.

2. Related works and other methods

The chapter presents selected methods and tools using the vibration signal as the main diagnostic parameter for monitoring the technical condition of machinery, especially vehicles. In addition, the authors have particularly focused on the description of methods for diagnostics of bearings as an element particularly susceptible to wear.

The paper [35] presents combustion engine valve clearance diagnostics based on vibration signals using machine learning algorithms. Vibration signals were obtained from a triaxial vibration acceleration transducers located on the engine head. The obtained time waveforms of vibration signals were parameterized for the engine working under different loads, with different rotational speeds and valve clearances. A similar approach using the improved variational mode decomposition (VMD) and bispectrum algorithm to analyze the vibration signal is described in the work [5]. The concept of vibration-based diagnostics of internal combustion engines is addressed in work [34]. The most important conclusion of the mentioned works is that it is possible to effectively use vibration signal analysis to evaluate valve clearance in a vehicle internal combustion engine.

Another approach representing the study of vibration signal for detecting sources of excitations in internal combustion engine is the paper [41]. The response signals caused by different excitations are coupled in the time and frequency domains. From the analyzed results, excitations that play a major role in the vibration signal in the context of different phases of engine operation have been identified. This is very useful information for monitoring the correct technical operation of an internal combustion engine. Another approach is presented in [7], where fault detection of diesel engine using vibration signal processing by combining rule-based algorithm and Bayesian networks (BNs) and Back Propagation neural networks (BPNNs) is proposed. The results of the research show the fault diagnosis method has a good diagnostic performance for a wide range of rotation speeds when the training data for BNs and BPNNs are from fixed speeds.

The paper [33] presents the possibility of diagnosing the upper suspension mount of a passenger car based on STFT vibration analysis. The evaluation of the condition is performed from the vehicle position at strictly defined EUSAMA test forces. The developed model allows to estimate the clearance in the mount.

The last example of research where not only vibration signal but mainly acoustic signal was used for machine diagnostics is the work [18]. The processing of vibroacoustic signals was based on the decomposition into several narrow-band spectral components applying different filter bank methods such as empirical mode decomposition, wavelet packet transform and Fourier-based filtering. Then, authors (based on selected measures) estimate the mutual statistical dependence between each component of signal and make the classification of various machine faults. As a result, the methodology is a promising algorithm to implement in condition monitoring of rotating machinery, even using measurements with low signal-to-noise ratio (for example acoustic signal).

Considering the above, the vibroacoustic signal is a very good carrier of machine diagnostic information. It is particularly useful for monitoring the technical condition of bearings, which is confirmed by studies [13, 15, 19, 21, 23, 40]. Analyses of the vibration signal in the frequency domain (e.g., determining the frequencies of characteristic failures of rolling bearing components [13, 21]) are an effective way to detect bearing malfunctions without disassembly. Fourier and Hilbert transforms [21, 40], wavelet transforms [15], and statistical tools in the form of various metrics (e.g., kurtosis, RMS, crest factor, etc.) [19, 23, 38] used in signal decomposition are also known ways to detect rotating element anomalies. The use of decision trees for rolling element bearing diagnostics based on time domain features of vibration signal is also frequently used. This topic is discussed in the works [1, 3, 22, 36]. The obtained results allow effective and fast technical condition diagnosis, but they are not verified in the conditions of real car operation.

Based on the selected literature analysis, the approach to monitoring the technical condition of road vehicle drive shaft bearings via vibration signal analysis was found to be very valid. An important aspect is the possibility to incorporate the low-cost method as one of many components of a comprehensive car self-diagnostic system (CSDS). The idea of diagnosing the technical condition of the vehicle from the position of the vehicle based on vibrations is also known in rail vehicles and presented, for example, in the works [12, 14, 27].

3. Research methodology

3.1. Main concept of the experimental measurements

The main research assumption was to perform vibration measurements of a drive shaft in a road vehicle, based on the assumptions of an active-passive experiment [9] (Figure 1). In the presented experiment, a qualitative assessment of the bearing after vibration tests was performed.

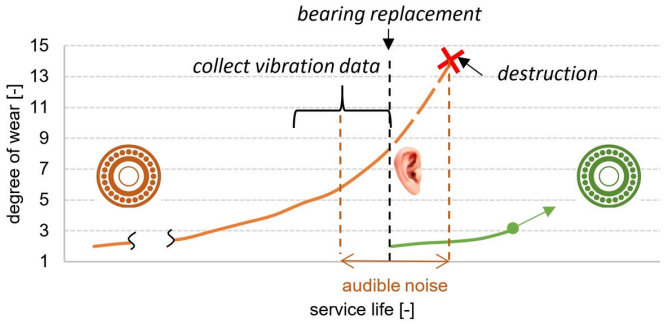

Fig. 1. The idea of the conducted active-passive experiment

The evaluation of the technical condition of the tested bearings was determined organoleptically by the technical team. This method is currently used by the operators. In this case, it is only possible to detect the degree of bearing disturbances in the noise phase, during which audible noise is emitted. This is the only reason why the bearing is currently qualified for replacement. However, detection of the malfunction is difficult at the beginning of this phase due to the relatively low noise level emission, especially in the vehicle interior. Once the malfunction was detected, vibration measurements of the bearing node were recorded under well-defined driving scenarios. The research material collected in this way formed the basis for further analysis to develop assumptions for diagnosing the bear-

ing node, eliminating the previous common approach. The developed method is to be a part of the CSDS – car self-diagnosis system. The user should receive information about bearing malfunctions from the vehicle cockpit.

The measurements were carried out in two test cases. In the first one, the vehicle was equipped with a worn bearing located in the supports of the vehicle drive shaft. In this case, the technical condition of the vehicle can be described as technically efficient and inoperative [25], i.e. the technical condition at the time instant before the bearing failure resulting from normal wear. Next, vibration measurements were conducted after replacing the worn bearing with a new and fully operational one. A total of 90 measurements were conducted, varying with the selected measurement scenarios. Table 1 shows the exact distribution of measurement scenarios, additionally highlighting the measurement data used for analysis and modeling (white background) and validation of results (blue background).

The most important differences concern the driving speeds of the vehicles, which are 40, 60, 80, 90, and 100 km/h, respectively. For each speed, 9 measurement series were carried out for both new and worn bearings. A single measurement was carried out in three vibration transmission axes and lasted for 5 s, during which a constant and unchanged driving speed was maintained.

The tests made use of relations resulting from the basic equations of technical diagnostics with observation of signals according to the implication [9]:

$$S(\Theta) = \Phi[(U(\Theta), E(\Theta), Z(\Theta)] \tag{1}$$

where: $S(\Theta)$ – signal parameters vector, $U(\Theta)$ – state parameters vector, $E(\Theta)$ – control parameters vector, $Z(\Theta)$ – disturbances, Θ – operating ageing measure, Φ – assignment operator.

During the experiment, the authors ensured a constant control vector $E(\Theta)$ comprising the constant driving speed within a given speed range (V_c), single driver driving style (R_s), constant technical condition of the other driving systems (T_s), quality of road surface (R_q), as-new condition of the tire tread (t_t), steady tire pressure (t_p):

$$E(\Theta) = \left[V_c \; R_s \; T_s \; R_q \; t_t \; t_p\right] \tag{2}$$

The possible influence of the disturbances $Z(\Theta)$ was minimized (mainly atmospheric conditions). Assuming $E(\Theta)$=*const.*, $Z(\Theta)$=*const.* and $Z(\Theta)$=*min.* the following relation was obtained:

$$U(\Theta) = S(\Theta) \tag{3}$$

This means that in order to assess the technical condition of a system, one needs to know the vector of the parameters of signals generated by this system and the influence on the measured signals will mainly have the change in the technical condition. Measurements were carried out in real traffic conditions, on a straight section of provincial road No. 241 (designated as the main road of accelerated traffic in Poland) with a length of about 3 km. The technical condition of the road is classified as good, characterized by a smooth asphalt surface, without visible and perceptible (while driving) road irregularities that would be an additional disturbance to the research process.

3.2. Research object and location of the measuring point

A Renault Kangoo car was used for the tests, the most important technical data of the vehicle are presented in Table 2.

The target vehicle component that was focused on during the experimental testing was the drive shaft, shown in Figure 2. The shaft is supported in two places (so-called supports), where SKF rolling bearings type 6006 RS were mounted. The outer diameter of the bearing is 55 mm, and the inner diameter is 30 mm.

After the first stage of measurements, the bearings on the supports were replaced in order to regenerate the shaft. The worn bearings were dismantled to perform an organoleptic examination and qualitative evaluation of wear and tear (Figure 3).

Table 1. Main information about measurement data

Bearing technical condition	Measurement series – 5 s each	Vehicle speed [km/h]				
		40	60	80	90	100
Bad	1	✓	✓	✓	✓	✓
	2	✓	✓	✓	✓	✓
	3	✓	✓	✓	✓	✓
	4	✓	✓	✓	✓	✓
	5	✓	✓	✓	✓	✓
	6	✓	✓	✓	✓	✓
	7	✓	✓	✓	✓	✓
	8	✓	✓	✓	✓	✓
	9	✓	✓	✓	✓	✓
Good	1	✓	✓	✓	✓	✓
	2	✓	✓	✓	✓	✓
	3	✓	✓	✓	✓	✓
	4	✓	✓	✓	✓	✓
	5	✓	✓	✓	✓	✓
	6	✓	✓	✓	✓	✓
	7	✓	✓	✓	✓	✓
	8	✓	✓	✓	✓	✓
	9	✓	✓	✓	✓	✓
Total = 90 measurement signals						

Table 2. Main technical data of the research object

Vehicle brand	Renault Kangoo
Combustion engine type	1.9 dCi (direct Common-rail injection)
Drivetrain type	4x4 attached automatically
Power	80 HP (59.66 kW)
Production year	2004
Mileage	300 000 km

Fig. 2. View of the drive shaft and the bearings location

Fig. 3. Wear of the main bearing elements: rolling elements, outer and inner raceways

Based on visual inspection, numerous damages in the form of pitting, scratches and flattening of the major rolling bearing components were found, as shown in Figure 3. The bearing components did not have a characteristic single crack or defect that could be the primary cause of bearing damage. This indicates their general wear from vehicle operation.

3.3. Measuring system and point location

During the measurements, vibration acceleration signals were recorded continuously in three directions with a sampling frequency of 65536 Hz in the frequency range up to 12 kHz. The vibration transducer was placed in the direct mounting area of the support on the differential side of the rear axle, as shown in Figure 4. The transducer was located on a flat surface as close as possible to the test bearing. This mounting arrangement provided a compromise between vibration transmission, measured frequency range, and interference. The measurements were conducted using a Hottinger Brüel & Kjaer triaxial vibration transducer type 4529-B-001 mounted to the vehicle using a dedicated magnet washer (Figure 4).

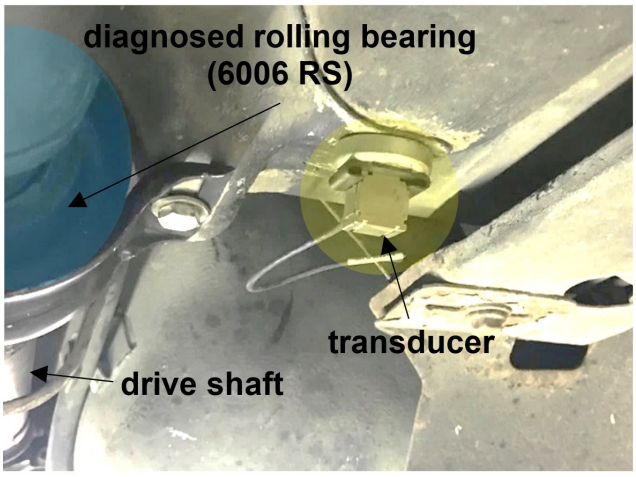

Fig. 4. Measurement point location

A Hottinger Brüel & Kjaer measurement module, type 3050-A-060, was used to acquire the measurement data. The measurement set prepared in this way allowed for individual control of vibration signal acquisition parameters, with synchronous recording and lossless archiving in digital form.

4. Analysis

In order to identify the vibration phenomena in the frequency domain, FFT analyses were performed for the extreme driving speeds. The obtained results were transformed from the time domain to the frequency domain using FFT analysis [28]:

$$X[k] = \sum_{n=0}^{N-1} x[n] e^{-i2\pi kn/N_p} \tag{4}$$

where: $X[k]$ - value of the FFT transform for k-th frequencies in the signal (amplitude, phase, complex number), N_p – number of signal samples, n – signal sample, x – signal value [m/s^2], k – current frequency (0 Hz to 6.4 kHz).

The analyses were performed with time weighting of Hanning window, with an overlap of 66.7%. Based on the obtained spectra, the main and dominant range of excited frequencies was determined. For this purpose, the effective values of vibration accelerations were calculated considering all measurement directions, as in the equation:

$$E\_RMS_{(f1,f2)} = \sqrt{\frac{1}{3}\sum_{y=1}^{3}\sqrt{\frac{1}{N}\sum_{i=1}^{N-1} a_{P_y,i}^2}} \tag{5}$$

where: N – number of signal samples, a_i – i–th signal amplitude of vibration acceleration, P_y – reference of the data to the measuring direction (P_1 – direction X, P_2 – direction Y, P_3 – direction Z), $f1$ -start of the frequency range, $f2$ – end of frequency range,

Figures 5–8 present the example results of case 4.

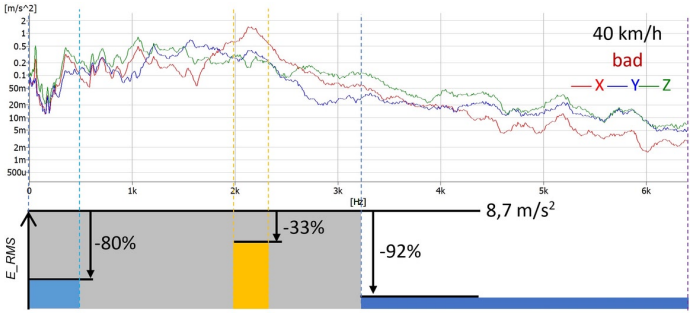

Fig. 5. Vibration acceleration spectrum of a faulty bearing node for case 4 at 40 km/h

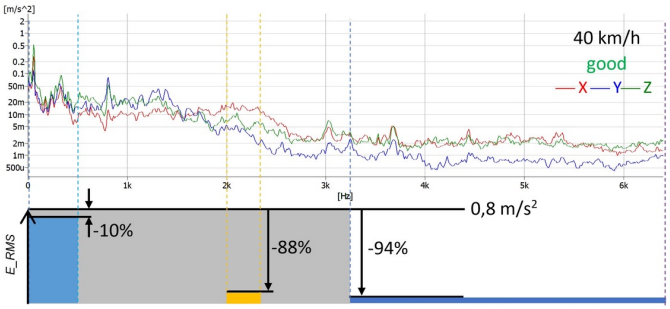

Fig. 6. Vibration acceleration spectrum of an efficient bearing node for case 4 at 40 km/h

The main range of excited frequencies for the bad bearing was in the frequency range up to 3.2 kHz. The calculated *RMS* of vibration acceleration filtered in this range was 8.7 m/s^2. However, the dominant

range was the 2-2.4 kHz range, for which the vibration acceleration was 33% lower compared to the main range. The 3.2-6.4 kHz range contained vibration acceleration that was 92% lower. For the good bearing, a different proportion of vibration was observed in the distinguished ranges. The dominant range was the low frequency range up to 500 Hz. This range contained 90% of the vibration acceleration from the main frequency range. In the case of vibration in the range 3.2-6.4 Hz, the vibration contribution was similar to that of the bad bearing. Moreover, in the 2-2.4 kHz range (dominant for the faulty bearing), the total vibration acceleration was 88% lower.

Similar percentage relations of particular frequency ranges between the bad and good case were also observed for the speed of 100 km/h. It should be noted that for the good bearing, the low frequency range up to 500 Hz did not have a dominant contribution to the acceleration in the range up to 3.2 kHz.

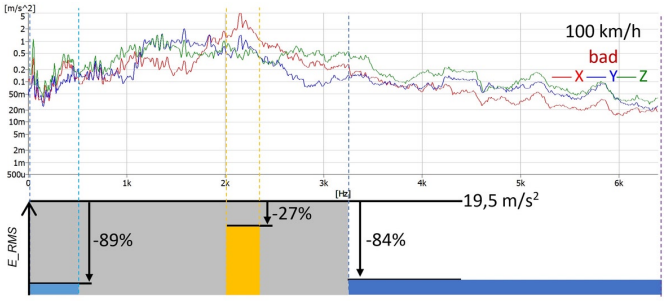

Fig. 7. Vibration acceleration spectrum of a faulty bearing node for case 4 at 100 km/h

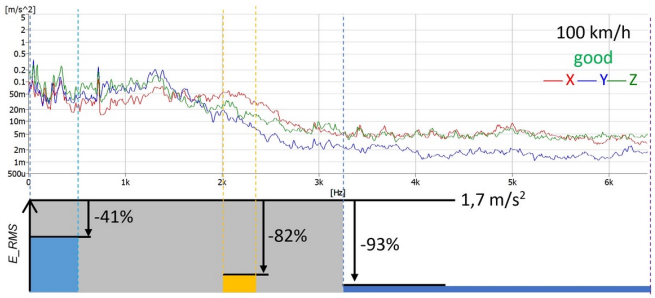

Fig. 8. Vibration acceleration spectrum of an efficient bearing node for case 4 at 100 km/h

In view of the results obtained, time domain features of vibration signal were calculated to develop a diagnostic parameter (also failure symptom). The most popular and proven measures in machine diagnostics were used [9] – root mean square (*RMS*), kurtosis (*K*) and skewness (*S*). The RMS value takes more into account the higher values of the instantaneous amplitude and is one of the most commonly used measures because it is proportional to the process power. Kurtosis, on the other hand, is a measure that is based on the density of the signal distribution, making it a very good parameter for rolling bearing diagnostics [19, 23, 38]. Finally, skewness can most generally be defined as a measure of asymmetry with respect to the mean value, by which it can also be used for machine fault analysis [20]. These measures were calculated according to the following equations [9]:

$$RMS = \sqrt{\frac{1}{N}\sum_{i=1}^{N-1} a_i^2} \tag{6}$$

$$K = \frac{\frac{1}{N}\sum_{i=1}^{N-1}(a_i - \bar{a})^4}{\left(\frac{1}{N}\sum_{i=1}^{N-1}(a_i - \bar{a})^2\right)^2} \tag{7}$$

$$S = \frac{\frac{1}{N}\sum_{i=1}^{N-1}(a_i - \bar{a})^3}{\sigma^3} \tag{8}$$

where: N – number of signal samples, a_i – i-th signal amplitude of vibration acceleration.

The above calculations were preceded by performing a combination of signal filtering. A total of 9 band-pass filters were created, of which 7 were associated with narrow frequency ranges up to 1000 Hz (NFR), and 2 were associated with wide frequency ranges (WFR). A schematic of the calculations along with the developed bandpass filters is shown in Figure 9.

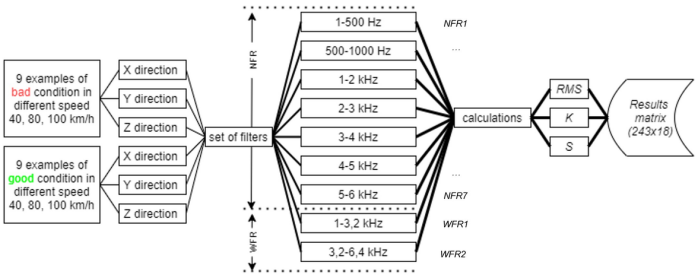

Fig. 9. Procedure for calculating time domain features of vibration acceleration signals

A total of 243 time domain features of vibration signal were obtained for each pass. The results thus obtained provided input to the problem of condition classification using machine learning in the form of decision trees. They are used to determine the affiliation of the results to classes of the qualitative dependent variable based on measurements of explanatory variables - predictors.

Decision tree is a graphical representation of recursive partitioning of a set of observations. This partitioning involved searching the feature space for all possible divisions of the dataset into two parts, so that at each successive step the division that results in the most strongly separated subsets is selected. Binary trees of the CART type were used in this analysis. The criteria for automatically stopping tree growth were based on a minimum number of objects in a leaf equal to 1.

In the analyses presented here, the qualitative dependent variable (categorical variable) classes were assigned a diagnostic condition (good/bad) and individual time domain features of vibration signal were assigned as explanatory variables (continuous variables). The algorithm used in the tree construction divided the classes in a way that minimized the prediction error (the least squares method). Figure 10 shows the division resulting from the decision tree analysis.

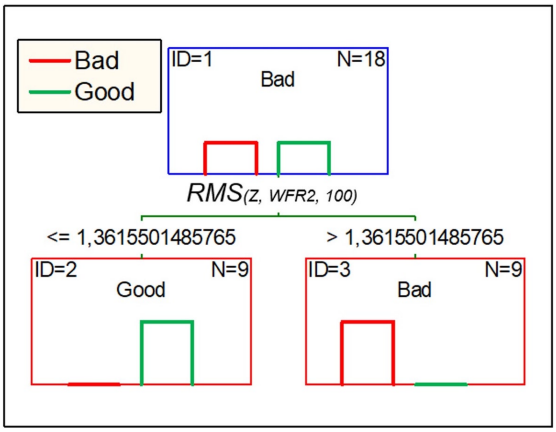

Fig. 10. Decision tree with selected diagnostic parameter

The use of a decision tree allowed the extraction of relevant measures, given the classes adopted. The best distribution of results ac-

cording to the condition was obtained using the RMS value from the vertical direction Z in the frequency range 3.2-6.4 kHz for the speed of 100 km/h. The value of the measure in the division of observations is 1.36 m/s^2 (D_v) for the damage cases analyzed. Thus, the performed analysis indicates that the differentiation of observations sets is most effective in higher frequency ranges in addition to the previously defined main ranges of dynamic excitations. The relative relationships between the D_v value and the mean values of the diagnostic parameter are shown in Figure 11.

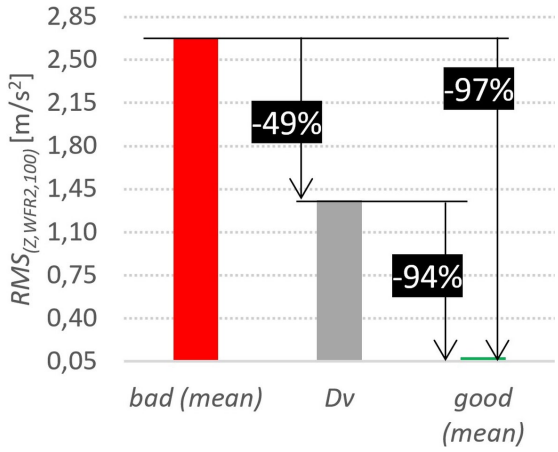

Fig. 11. Relationship between the D_v value and the mean values of the diagnostic parameter

The selected measure $RMS_{(Z,\ WFR2,\ 100)}$ will be used as a diagnostic parameter for the bearings technical condition. Considering only the vertical direction Z is the basis for reducing the applied vibration transducer from triaxial to uniaxial, which will affect the unit cost of the system. The results of $RMS_{(Z,\ WFR2,\ 100)}$ against the background of the studied cases are presented in Figure 12.

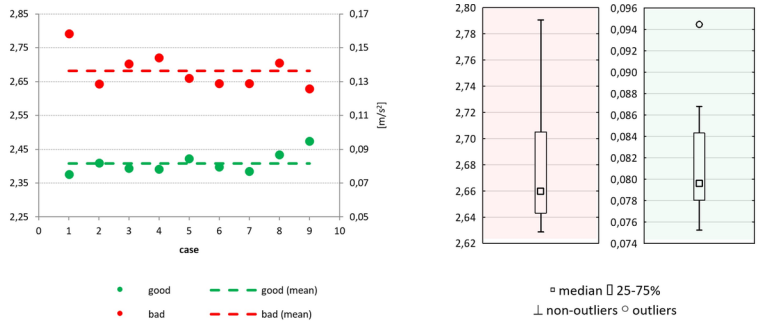

Fig. 12. The value of $RMS_{(Z,\ WFR2,\ 100)}$ parameter for the extreme driving speed cases studied (left) with statistical visualization of the results (right)

The spread of the data for a good bearing is about 0.02 m/s^2, and for a bad bearing it is 10 times larger, i.e. about 0.2 m/s^2. The median parameter for the faulty bearing is 2.66 m/s^2, and for the efficient bearing it is 97% smaller (0.08 m/s^2). Pearson correlation coefficient was calculated between the speed and $RMS_{(Z,\ WFR2,\ 100)}$, according to the equation:

$$r(x,y)=\sum_{i=1}^{N}\frac{(x_i-\bar{x})(y_i-\bar{y})}{\sqrt{\sum_{i=1}^{N}(x_i-\bar{x})^2}\sqrt{\sum_{i=1}^{N}(y_i-\bar{y})^2}} \tag{9}$$

where: N – sample size, x, y – the individual sample points indexed with i, $\bar{x}$, $\bar{y}$ – sample mean.

The resulting Pearson correlation coefficient was $r(V,\ RMS_{(Z,\ WFR2,\ 100)})$=0,98 which shows a strong correlation with driving speed.

For the developed parameter $RMS_{(Z,\ WFR2,\ 100)}$ the authors created models for the assessment of the technical state of the bearings. A total of four different regression models were examined, including the polynomial, gaussian and exponential ones. Figure 13 presents the above-mentioned models.

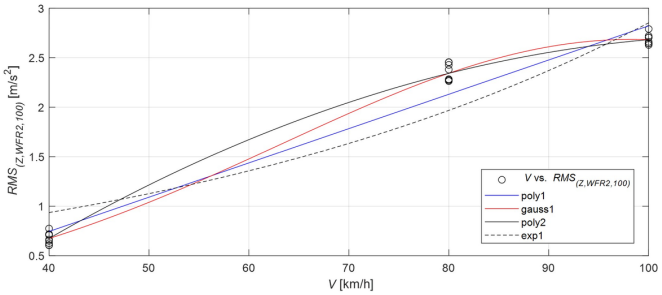

Fig. 13. The developed regression models of the parameter $RMS_{(Z,\ WFR2,\ 100)}$ of a faulty bearing as a function of driving speed.

The equations of the models are shown below:

$$f_{poly1} = -0.03464x - 0.64108 \tag{10}$$

$$f_{gauss1} = 2.6848e^{-\left(\frac{x-98.35}{49,632}\right)^2} \tag{11}$$

$$f_{poly2} = -0.00041154x^2 - 0.09108x - 2.31107 \tag{12}$$

$$f_{exp1} = 1.0312e^{(-0.15948x)} \tag{13}$$

The regression models must be subjected to statistical validation. The models were validated by determining a series of statistical data. First, the fitness level of the models to the actual data was determined. For this reason, a coefficient of determination R^2 was obtained. In order to determine the significance of individual coefficients of regression, the authors proposed the following hypotheses:

$$H_0 : \beta_j = 0 \tag{14}$$

$$H_1 : \beta_j \neq 0 \tag{15}$$

Rejecting H_0 signifies that authors have statistical grounds to state that there exists a correlation between the dependent variable and at least one independent variable. For the testing of the hypotheses related to the determination of the statistical significance of individual coefficients of regression, the authors used a t-Student distribution. In the investigations, the authors adopted a statistical significance on the level of α=0.05. The results of the statistical analysis including root mean square error (RMSE) and coefficient of determination (R^2) of each model have been presented in Table 3.

When analyzing the results in Table 3, the authors have observed that all the models respectively, contained statistically insignificant coefficients, which is why these models were eliminated from further investigations. The authors assumed that they would select a model of regression, for which the coefficient of determination is equal or greater than 0.90, has the lowest *RMSE* value out of all the models and its model coefficients are statistically significant. Such assumptions are met by the models gauss1 and poly2. The obtained coefficients indicate these models can accurately forecast the data. Finally, the authors selected the poly2 model.

Table 3. Statistical analysis results of the models of the parameter $RMS_{(Z, WFR2, 100)}$

	poly1		gauss1		poly2		exp1	
RMSE	0.171		0.0668		0.0668		0.3	
R^2	0.965		0.995		0.995		0.888	
Estimated coefficient in model (EC)	EC	p-value	EC	p-value	EC	p-value	EC	p-value
1st coefficient	0.03464	1.0686E-19	2.6848	5.9872E-36	-0.00041154	1.6124E-11	0.44513	1.1543E-06
2nd coefficient	-0.64108	1.5056E-06	98.35	7.3189E-32	0.09108	5.604E-16	0.01858	6.2325E-11
3rd coefficient	–	–	49.632	6.5052E-24	-2.31107	3.5702E-14	–	–

5. Validation of the diagnostic parameter model

The validation of the developed model was based on the results for intermediate driving speeds, i.e. 60 km/h and 90 km/h. The measurements were carried out in the same way as for the remaining speeds, by making 9 series. For these speeds, $RMS_{(Z, WFR2, 100)}$ parameter value was predicted using equation (11). The results as a function of driving speed are shown in Figure 14.

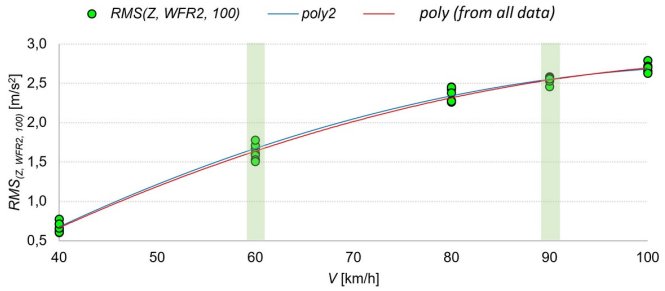

Fig. 14. The value of $RMS_{(Z, WFR2, 100)}$ parameter as a function of speed together with validation data

For the data obtained, the prediction error (PE) was calculated according to the equation:

$$PE = \frac{\left|x_{a,i} - x_{m,i}\right|}{x_{m,i,j}} \tag{16}$$

where: x_a – the value of $RMS_{(Z, WFR2, 100)}$ from measurements, x_m – estimated value of $RMS_{(Z, WFR2, 100)}$ from the model, i – i-th measurement.

The results of the statistical analysis of the prediction error (PE) are shown in Figure 15.

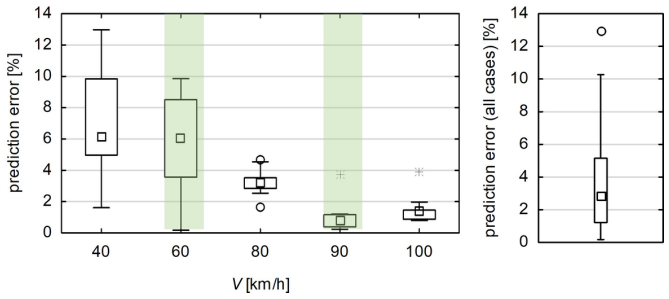

Fig. 15. Prediction error results for individual driving speeds

The largest prediction errors in model validation are for speeds of 60 km/h and in the range of 0.2–9.9%. For the 90 km/h validation speed, the error range was 0.2–1.2% with a single case of extreme observation error of 3.6%. The prediction error range of the model when all data (baseline and validation) were considered in the category of non-outlier observations 0.2–10.3%. Individually, an error of 13.0% defined as an outlier was observed. Figure 16 shows the mean prediction error for a given speed.

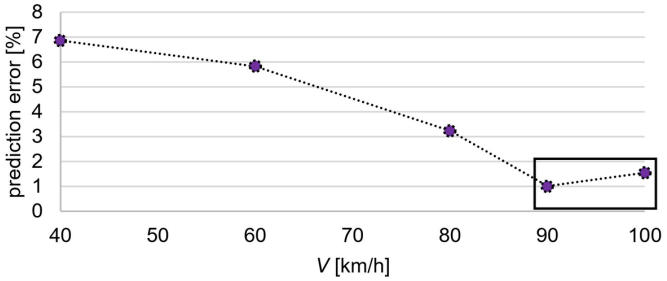

Fig. 16. Mean prediction error as a function of driving speed

As can be seen from the data presented in Figure 16, the mean prediction error is smallest for the two highest driving speeds, being 1-1.6%. The presented results are therefore an additional motivation to carry out diagnostic tests of the bearing condition at 100 km/h.

6. Diagnostic parameter limit value

In the next stage of the work, the evaluation criteria for the developed diagnostic parameter $RMS_{(Z, WFR2, 100)}$ were established. The number of bearing node conditions W_p was determined based on a three-value condition assessment using the following classes [9, 25]:

$$W_p = \left\{w^1, w_n^1, w^0\right\} \tag{17}$$

where: W_p – set of technical conditions for traction transmission diagnostics, w^1 - class of good technical conditions, w_n^1 - class of average technical conditions (permissible), w^0 – class of bad technical conditions. The w^1 technical condition means that the value of the diagnostic parameter y did not reach and did not exceed the upper limit value Sg. The w^0 technical condition is reached when the value of a diagnostic parameter reaches or exceeds the limit value. In contrast, an unacceptable condition w_n^1 means that the diagnostic parameter has reached or exceeded the down limit value but has not reached the upper limit value. The relationship between the diagnostic parameter and the conditions can be represented as follows:

$$RMS_{(Z,WFR2,100)} \leq Sg \rightarrow w^1 \tag{18}$$

$$Sg > RMS_{(Z,WFR2,100)} \geq Sd \rightarrow w_n^1 \tag{19}$$

$$RMS_{(Z,WFR2,100)} \geq Sg \rightarrow w^0 \tag{20}$$

Continued operation of an object that has reached a condition w^0 is not economically, technically and environmentally advisable.

Due to the availability of data related to the damaged bearing, it was decided to use an upper limit value estimation method based on the mean pre-failure value of the symptom. Upper limit value (also breakdown value) (*Sg*) and down limit value (also alarm value) (*Sd*) was determined according to equations:

$$Sg = \bar{x}_w - k\sigma \tag{21}$$

$$Sd = Sg - k\sigma \tag{22}$$

where: *Sg* – upper limit value of diagnostic parameter *Sd* – down limit value of diagnostic parameter, $\bar{x}_w$ – mean failure value of a diagnostic parameter, *k* – degradation factor. The factor *k*=3 was selected *a priori*.

With a large set of pre-failure data, the Cempel method [8], which is a modification of the Neyman-Pearson method [9, 10], is recommended for determining evaluation criteria. In this method, an acceptable level of unnecessary overhauls is assumed when determining the upper limit value *A* [8, 43]. An erroneous overhaul decision will occur when the diagnostic parameter of an object in a serviceable condition exceeds the value of *Sg*. The total probability of such an event is equal to the product of the readiness factor *P(z)* and the probability of exceeding *Sg* in a good technical condition [9].

The calculated upper limit value and down limit value are respectively *Sg*=2,52 m/s^2 and *Sd*=2,37 m/s^2. These are shown against the results obtained in Figure 17. The majority (8/9 cases) of the values of diagnostic parameter $RMS_{(Z,\ WFR2,\ 100)}$ for the bad technical condition of the bearings is above the upper limit value *Sg*, which indicates the correct classification into the condition w^0 due to the actual technical condition confirmed by the vision tests. When the results of the new bearing are related to the upper limit value, it can be observed that they represent 3.5% of its value.

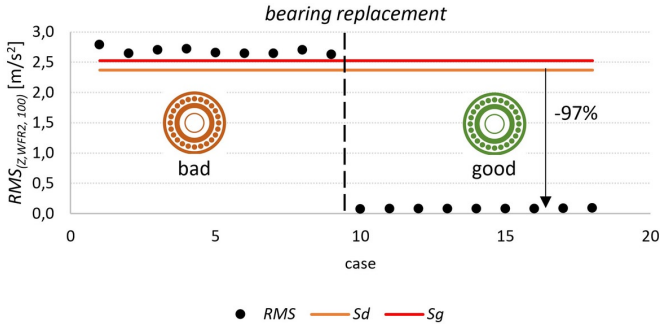

Fig. 17. Upper limit value and down limit value against measurement results

The algorithm for diagnosing the drive shaft is shown in Figure 18.

The diagnostic algorithm assumes first of all monitoring the current driving speed. In the case of detection of reaching the speed of 100 km/h, a five-second measurement of vibration accelerations from the bearing node is triggered. This measurement should be synchronous with the measurement of the driving speed in order to be able to assess the condition of a constant driving speed. The steady speed is met when the speed standard deviation is less than 2 km/h. After meeting the assumed requirements, the value of the diagnostic parameter $RMS_{(Z,\ WFR2,\ 100)}$ is calculated and compared with the evaluation criteria. Exceeding the upper limit value is equivalent to displaying a message to the driver to replace the bearing. If the down limit value is exceeded, the driver is informed of the need to purchase a new bearing for its later replacement. Moreover, the information related to the monitoring of the diagnostic parameter can be used as input data for the maintenance systems of technical objects, taking into account the results of the risk analysis [16].

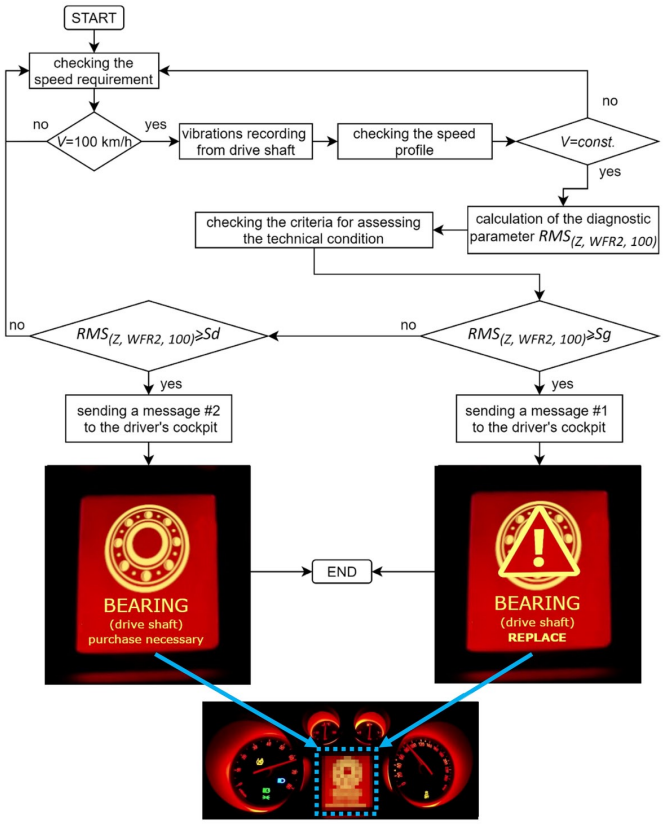

Fig. 18. The algorithm for diagnosing the drive shaft bearing

7. Summary and conclusions

Based on the study, an effective tool was developed to evaluate the technical condition of bearings in the drive shaft support of a passenger car. The use of vibration signal for technical diagnostics of bearings is well known, but most of the work is carried out in steady-state conditions using stationary machines (e.g., production machines). In this case, the distinctive feature of the present work is carrying out experimental tests on a vehicle (based on the assumptions of the active-passive experiment) in real conditions. This makes it possible to effectively implement the developed diagnosis algorithm as a component of a broader, comprehensive car self-diagnostic system called CSDS. The assumptions of the CSDS system are related to the absolution of the concept of OBD systems by diagnosing the key elements from the point of view of driving safety and vehicle service cost planning.

In the presented method, the key issue was to identify the frequency distribution of the vibration acceleration signal. On its basis, a set of filters and time domain features of vibration signal was created to describe vibration phenomena in order to select the most sensitive diagnostic parameter to the change of technical condition. For this purpose, the decision tree algorithm was used to extract relevant measures due to the adopted classes of technical condition. The selected diagnostic parameter is the RMS value measured at 100 km/h in a wide frequency range beyond 3.2 kHz, i.e. outside the main vibration range resulting from the vehicle dynamic phenomena. It is worth noting that for other speeds, it is also possible to adapt the selected diagnostic process. Next, the parameter evaluation criteria were determined by calculating the upper limit values and down limit values. The main purpose of the developed diagnostic algorithm is to inform the user of the vehicle about the necessity of bearing replacement or to alert the driver to impending damage (wear) and the need to plan for the purchase of a new bearing.

In future research directions, the authors will focus on developing a full speed range for the diagnostic process. In addition, the goal is to implement this type of tool into a number of other on-board diagnostic subsystems, which is not associated with high costs, and can bring

tangible benefits of quickly responding to impending malfunctions of elements susceptible to wear in a road vehicle.

Acknowledgements

All presented work is partly funded by Statutory Activities fund of the Institute of Transport, PUT (PL) 0416/SBAD/0003.

References

1. Abid F Ben, Sallem M, Braham A. Optimized SWPT and Decision Tree for Incipient Bearing Fault Diagnosis. 2019 19th International Conference on Sciences and Techniques of Automatic Control and Computer Engineering (STA), IEEE: 2019: 231-236, https://doi.org/10.1109/STA.2019.8717197.
2. Ahmed U, Ali F, Jennions I. A review of aircraft auxiliary power unit faults, diagnostics and acoustic measurements. Progress in Aerospace Sciences 2021; 124: 100721, https://doi.org/10.1016/j.paerosci.2021.100721.
3. Amarnath M, Sugumaran V, Kumar H. Exploiting sound signals for fault diagnosis of bearings using decision tree. Measurement 2013; 46(3): 1250-1256, https://doi.org/10.1016/j.measurement.2012.11.011.
4. Andria G, Attivissimo F, Di Nisio A et al. Development of an automotive data acquisition platform for analysis of driving behavior. Measurement: Journal of the International Measurement Confederation 2016; 93: 278-287, https://doi.org/10.1016/j.measurement.2016.07.035.
5. Bi X, Cao S, Zhang D. Diesel Engine Valve Clearance Fault Diagnosis Based on Improved Variational Mode Decomposition and Bispectrum. Energies 2019; 12(4): 661, https://doi.org/10.3390/en12040661.
6. Borucki S, Cichoń A, Majchrzak H, Zmarzły D. Evaluation of the Technical Condition of the Active Part of the High Power Transformer Based on Measurements and Analysis of Vibroacoustic Signals. Archives of Acoustics 2017; 42(2): 313-320, https://doi.org/10.1515/aoa-2017-0033.
7. Cai B, Sun X, Wang J et al. Fault detection and diagnostic method of diesel engine by combining rule-based algorithm and BNs/BPNNs. Journal of Manufacturing Systems 2020; 57: 148-157, https://doi.org/10.1016/j.jmsy.2020.09.001.
8. Cempel C. Limit value in the practice of machine vibration diagnostics. Mechanical Systems and Signal Processing 1990; 4(6): 483-493, https://doi.org/10.1016/0888-3270(90)90047-O.
9. Cempel C. Vibroacoustic condition monitoring (Ellis Horwood Series in Mechanical Engineering). Warsaw, Ellis Horwood: 1993.
10. Cempel C. Vibroacoustical diagnostics of machinery: An outline. Mechanical Systems and Signal Processing 1988; 2(2): 135-151, https://doi.org/10.1016/0888-3270(88)90039-8.
11. Corni I, Symonds N, Wood R J K et al. Real-time on-board condition monitoring of train axle bearings. Stephenson Conference Research for Railways 2015 2015; (17): 477-489.
12. Czechyra B, Firlik B. On-line monitoring system of the technical condition of the infrastructure and running gear of a light rail vehicle (in Polish). Communication Review 2014; 2: 6-10.
13. Donelson J, Dicus R L. Bearing defect detection using on-board accelerometer measurements. ASME/IEEE 2002 Joint Rail Conference, RTD 2002 2002: 95-102, https://doi.org/10.1115/RTD2002-1645.
14. Firlik B, Czechyra B, Chudzikiewicz A. Condition monitoring system for light rail vehicle and track. Key Engineering Materials 2012; 518: 66-75, https://doi.org/10.4028/www.scientific.net/KEM.518.66.
15. Gharesi N, Arefi M M, Ebrahimi Z et al. Analyzing the Vibration Signals for Bearing Defects Diagnosis Using the Combination of SGWT Feature Extraction and SVM. IFAC-PapersOnLine 2018; 51(24): 221-227, https://doi.org/10.1016/j.ifacol.2018.09.581.
16. Gill A. Optimisation of the technical object maintenance system taking account of risk analysis results. Eksploatacja i Niezawodnosc – Maintenance and Reliability 2017; 19(3): 420-431, https://doi.org/10.17531/ein.2017.3.13.
17. 10 Problems Cars Can Diagnose By Themselves. [https://auto.howstuffworks.com/under-the-hood/trends-innovations/10-problems-cars-can-diagnose-themselves.htm].
18. Holguín-Londoño M, Cardona-Morales O, Sierra-Alonso E F et al. Machine Fault Detection Based on Filter Bank Similarity Features Using Acoustic and Vibration Analysis. Mathematical Problems in Engineering 2016, https://doi.org/10.1155/2016/7906834.
19. Immovilli F, Cocconcelli M, Bellini A, Rubini R. Detection of generalized-roughness bearing fault by spectral-kurtosis energy of vibration or current signals. IEEE Transactions on Industrial Electronics 2009; 56(11): 4710-4717, https://doi.org/10.1109/TIE.2009.2025288.
20. Kaul S. Crack diagnostics in beams using wavelets, kurtosis and skewness. Nondestructive Testing and Evaluation 2014; 29(2): 99-122, https://doi.org/10.1080/10589759.2013.854783.
21. Liu H, Li D, Yuan Y et al. Fault diagnosis for a bearing rolling element using improved VMD and HT. Applied Sciences 2019, https://doi.org/10.3390/app9071439.
22. Liu N, Liu B, Xi C. Fault diagnosis method of rolling bearing based on the multiple features of LMD and random forest. IOP Conference Series: Materials Science and Engineering 2020, https://doi.org/10.1088/1757-899X/892/1/012068.
23. Lorenzo F De, Calabro M. Kurtosis : A Statistical Approach to Identify Defect in Roller Bearings. 2nd International Conference on Marine Research and Transportation 2007; 3: 17-24.
24. Merkisz J, Rychter M. Basic proceeding of diagnosis and strategy of decision on OBD II system. AVEC - International Symposium on Advanced Vehicle Control, Hiroshima, 2002.
25. Niziński S, Michalski R. Diagnostics of technical objects (in Polish). Radom (Poland), ITeE: 2002.
26. Nowakowski T, Komorski P, Szymański G M, Tomaszewski F. Wheel-flat detection on trams using envelope analysis with Hilbert transform. Latin American Journal of Solids and Structures 2019, https://doi.org/10.1590/1679-78255010.
27. Nowakowski T, Motyl M, Babiak A. Simplified diagnostics of the drive system in the operation of a rail vehicle. Railway Reports 2019; 2(182): 49-54, https://doi.org/10.36137/1824p.
28. Randall R B, Tech B. Frequency analysis. Brüel & Kjær: 1987.
29. Sankavaram C, Kodali A, Pattipati K R, Singh S. Incremental classifiers for data-driven fault diagnosis applied to automotive systems. IEEE Access 2015; 3: 407-419, https://doi.org/10.1109/ACCESS.2015.2422833.
30. Sawczuk W, Szymański G M. Diagnostics of the railway friction disc brake based on the analysis of the vibration signals in terms of resonant

frequency. Archive of Applied Mechanics 2017; 87(5): 801-815, https://doi.org/10.1007/s00419-016-1202-0.
31. Smith C, Akujuobi C M, Hamory P, Kloesel K. An approach to vibration analysis using wavelets in an application of aircraft health monitoring. Mechanical Systems and Signal Processing 2007; 21(3): 1255-1272, https://doi.org/10.1016/j.ymssp.2006.06.008.
32. Soy H, Toy I. Design and implementation of smart pressure sensor for automotive applications. Measurement: Journal of the International Measurement Confederation 2021, https://doi.org/10.1016/j.measurement.2021.109184.
33. Szymański G M, Josko M, Tomaszewski F, Filipiak R. Application of time-frequency analysis to the evaluation of the condition of car suspension. Mechanical Systems and Signal Processing 2015; 58-59: 298-307, https://doi.org/10.1016/j.ymssp.2014.12.017.
34. Szymański G. Problems in diagnostics of internal combustion engines with the use of resonance vibrations (in Polish). Poznan, Poznan University of Technology: 2013.
35. Szymański G M, Tabaszewski M. Engine valve clearance diagnostics based on vibration signals and machine learning methods. Eksploatacja i Niezawodnosc – Maintenance and Reliability 2020; 22(2): 331-339, https://doi.org/10.17531/ein.2020.2.16.
36. Tabaszewski M. Identification of rolling bearing condition by means of a classification tree. Vibrations in Physical Systems 2019; 30(2): 1-8.
37. Theissler A, Pérez-Velázquez J, Kettelgerdes M, Elger G. Predictive maintenance enabled by machine learning: Use cases and challenges in the automotive industry. Reliability Engineering and System Safety 2021; 215: 107864, https://doi.org/10.1016/j.ress.2021.107864.
38. Wang H, Chen P. Fault diagnosis method based on kurtosis wave and information divergence for rolling element bearings. WSEAS Transactions on Systems 2009; 8(10): 1155-1165.
39. Wu J Da, Liao S Y. A self-adaptive data analysis for fault diagnosis of an automotive air-conditioner blower. Expert Systems with Applications 2011; 38(1): 545-552, https://doi.org/10.1016/j.eswa.2010.06.100.
40. Yu D, Cheng J, Yang Y. Application of EMD method and Hilbert spectrum to the fault diagnosis of roller bearings. Mechanical Systems and Signal Processing 2005; 19(2): 259-270, https://doi.org/10.1016/S0888-3270(03)00099-2.
41. Zhao X, Yang Z, Pan B et al. Analysis of excitation source characteristics and their contribution in a 2-cylinder diesel engine. Measurement: Journal of the International Measurement Confederation 2021; 176(February): 109195, https://doi.org/10.1016/j.measurement.2021.109195.
42. Zhao Y, Liu P, Wang Z et al. Fault and defect diagnosis of battery for electric vehicles based on big data analysis methods. Applied Energy 2017; 207: 354-362, https://doi.org/10.1016/j.apenergy.2017.05.139.
43. Żółtowski B, Łukasiewicz M. Machine vibration diagnostics (in Polish). Bydgoszcz, Scientific Publisher of the Institute of Sustainable Technologies - National Research Institute: 2012.